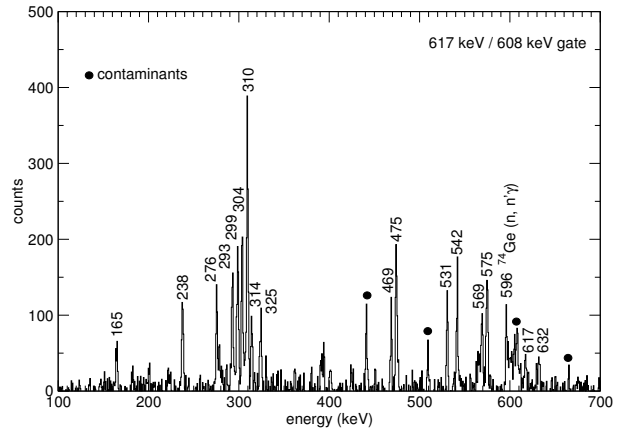
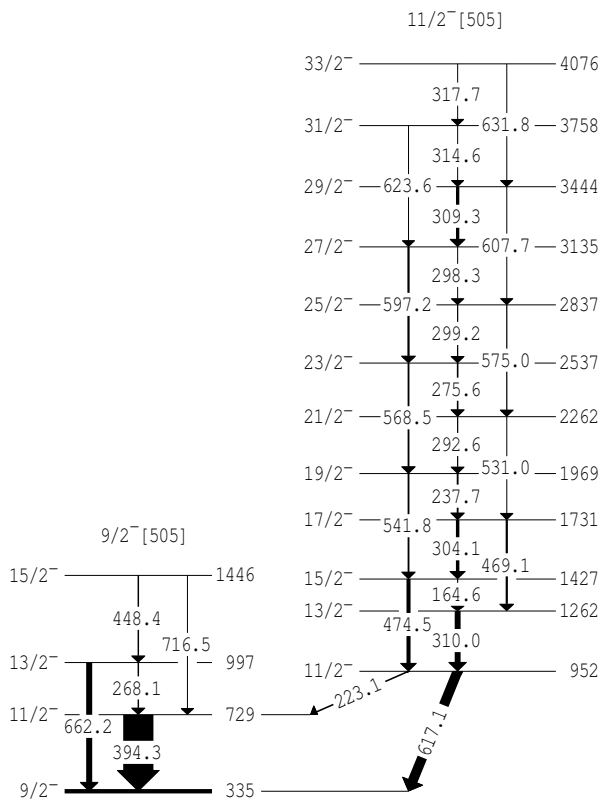


**Fig. 2.** Coincidence spectrum double-gated on the 394.3 and 831.8 keV  $\gamma$ -rays, showing transitions in the unfavoured signature of the prolate  $h_{9/2}$  structure.



**Fig. 4.** Coincidence spectrum double-gated on the 617.1 and 607.7 keV  $\gamma$ -rays, showing transitions in the  $11/2^-$  [505] band.



**Fig. 3.** Partial level scheme of  $^{187}\text{Tl}$  showing the  $11/2^-$  [505] band and its decay to the  $9/2^-$  [505] band.

function of the transition mixing ratio  $\delta$ , assuming spins of  $11/2$  (left panel) and  $13/2$  (right panel) for the 952 keV state. The measured lifetime limit for the 952 keV state from  $\gamma - \gamma$  time differences is  $\tau < 3$  ns.

For a spin of  $13/2$ , minima at  $\delta \rightarrow \pm\infty$  are seen for the 617.1 keV transition. This would imply it was either a pure  $M3$  or  $E3$  transition, with unphysical transition strengths of  $> 5.4(4) \times 10^5$  or  $> 6.3(4) \times 10^3$  W. u. respectively. Looking at the other solutions for  $\delta$  gives the limits on the transition strengths shown in Table 1. From the values for the  $M2$  components, the 952 keV state cannot have  $J^\pi = 11/2^+$  or  $13/2^+$ .

In order to decide between the  $J^\pi = 11/2^-$  and  $13/2^-$  possibilities, expected values of the intensity ratio between

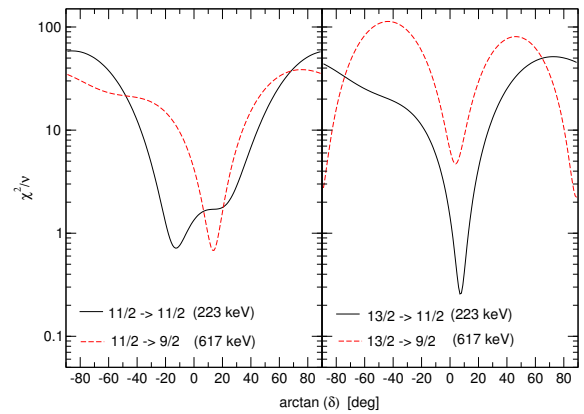


**Fig. 5.** Angular distribution  $\chi^2$  analysis for the 223.1 and 617.1 keV transitions.

**Table 1.** Transition strengths of the 223.1 and 617.1 keV  $\gamma$ -rays for various spins and parities of the 952 keV state.

$J^\pi$	$E_\gamma$ (keV)	$X\lambda$	$I_\gamma$	$\alpha_T$	Trans. Strength (W. u.)
$11/2^-$	223.1	$M1$	$24(7)^a$	0.887	$> 9(4) \times 10^{-5}$
	223.1	$E2$	$2.0(6)^a$	0.282	$> 6(2) \times 10^{-2}$
	617.1	$M1$	$184(57)^b$	0.0572	$> 3(1) \times 10^{-5}$
	617.1	$E2$	$3(1)^b$	0.0173	$> 6(3) \times 10^{-4}$
$11/2^+$	223.1	$E1$	$24(7)^a$	0.0581	$> 10(4) \times 10^{-7}$
	223.1	$M2$	$2.0(6)^a$	4.01	$> 7(3)$
	617.1	$E1$	$184(57)^b$	0.0060	$> 4(2) \times 10^{-7}$
	617.1	$M2$	$3(1)^b$	0.156	$> 7(3) \times 10^{-2}$
$13/2^-$	223.1	$M1$	$26(1)^c$	0.887	$> 1.0(1) \times 10^{-4}$
	617.1	$E2$	$187(9)^c$	0.0173	$> 3.7(2) \times 10^{-2}$
$13/2^+$	223.1	$E1$	$26(1)^c$	0.0581	$> 9.6(6) \times 10^{-7}$
	617.1	$M2$	$187(9)^c$	0.156	$> 3.9(3)$

<sup>a</sup>  $I_\gamma$  deduced using  $\delta = -0.23(7)$  from the angular distribution.

<sup>b</sup>  $I_\gamma$  deduced using  $\delta = 0.13(4)$  from the angular distribution.

<sup>c</sup>  $I_\gamma$  deduced using  $\delta \approx 0$  from the angular distribution.

the 223.1 and 617.1 keV  $\gamma$ -rays have been calculated assuming that the transitions are pure  $M1$  ( $11/2^-$ ) or  $M1$  and  $E2$  ( $13/2^-$ ) with all the strengths being 1 W.u. These values are compared to the measured branching ratio (see Table 2). The expected branching ratio for the  $J^\pi = 11/2^-$  possibility agrees with the measured value, but for the  $J^\pi = 13/2^-$  case, the expected ratio is more than  $\sim 350$  times

**Table 2.** Ratio of observed  $\gamma$ -ray intensities for the 223.1 and 617.1 keV transitions compared with the expected values for alternative spin assumptions for the 952 keV state (see text for further details).

$J^\pi$	$I_\gamma(617.1)/I_\gamma(223.1)$ [measured]	$I_\gamma(617.1)/I_\gamma(223.1)$ [expected]
$11/2^-$	7.2(5)	20(13)
$13/2^-$	7.2(5)	0.020(2)

less than the measured value. Hence, the 952 keV level is assigned the spin of  $11/2^-$ , consistent with it being the  $11/2^-$  [505] bandhead that is expected at low excitation energy.

### 3 Discussion

#### 3.1 The unfavoured signature of the $h_{9/2}$ band

The alignment of the single-particle angular momentum to the rotation axis,  $i_x$ , can be obtained by subtracting the (parametrised) rotational angular momentum of the collective core. Figure 6 plots the alignments for the  $h_{9/2}$  bands in  $^{187}\text{Tl}$ ,  $^{183}\text{Au}$  and  $^{185}\text{Au}$  as a function of the rotational frequency  $\hbar\omega$ . The reference parameters that are used,  $\mathcal{I}_0 = 27 \text{ MeV}^{-1}\hbar^2$  and  $\mathcal{I}_1 = 190 \text{ MeV}^{-3}\hbar^4$ , are the same as those used in Ref. [12], where they were chosen to produce  $i_x \approx 0$  for the prolate cores of even-even mercury nuclei around  $N=104$  (see, for example, Fig. 2 in Ref [12] and Fig. 7 below).

In an odd-mass nucleus, a difference of  $\sim 1\hbar$  is expected between the alignments of the favoured and unfavoured signatures of a rotational band when the Fermi level is close to the  $\Omega = 1/2$  orbital of a high- $j$  particle, so that the odd particle is fully aligned to the rotation axis [8]. Hence, the rotation-aligned  $h_{9/2}$  proton in  $^{187}\text{Tl}$ , which mainly occupies the  $\pi 1/2^-$  [541] and  $\pi 3/2^-$  [532] orbitals that are close to the Fermi level, should result in two rotational sequences with  $\Delta i_x \approx 1\hbar$ .

The alignments of the two negative-parity bands in  $^{187}\text{Tl}$  in Figure 1, one of them being the known “ $h_{9/2}$ ” band, are in the top panel, and they display a similar behaviour to the  $h_{9/2}$  bands in  $^{183}\text{Au}$  and  $^{185}\text{Au}$  that are shown in the lower panels. Therefore, the new structure feeding the known “ $h_{9/2}$ ” band is deduced to be the unfavoured signature.

#### 3.2 Deformation of the prolate $h_{11/2}$ structure

Ref. [12] discusses how differences in the slopes and magnitude of alignments can be used to investigate relative deformations. For example,  $^{188}\text{Pb}$  appears to have a slightly lower deformation compared to  $^{180,182,184}\text{Hg}$  based upon its lower alignment (see Figure 2 in Ref. [12] and Figure 7 here). Similarly, the alignment of  $^{186}\text{Hg}$  is less than  $^{184}\text{Hg}$  at low spin. Also plotted is the alignment of the  $11/2^-$  [505] band in  $^{187}\text{Tl}$ , which seems to have a similar deformation to the prolate  $^{186}\text{Hg}$  core (bottom panel), despite the previous calculation that predicted the  $11/2^-$  [505] state in  $^{187}\text{Tl}$  should have a lower deformation [3].

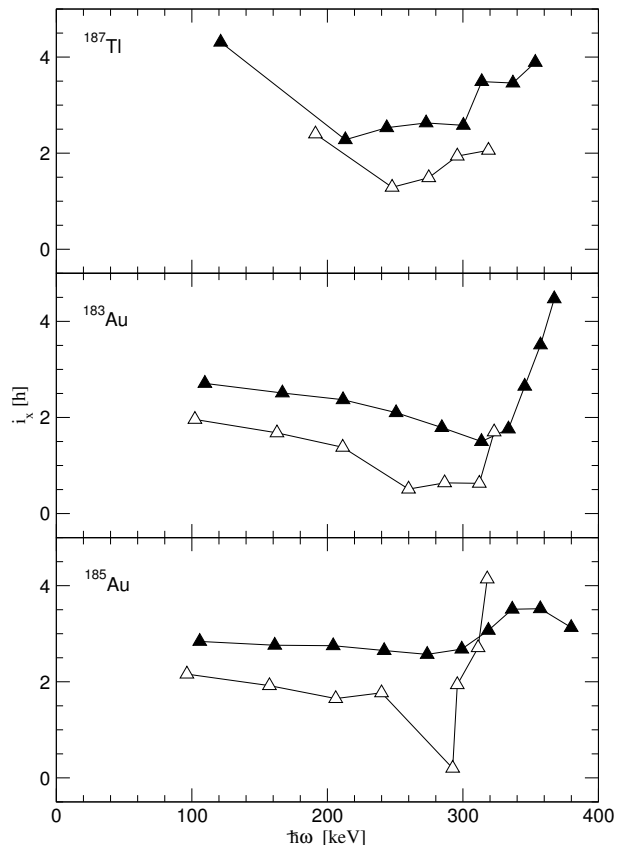


**Fig. 6.** Comparison of alignments for the prolate  $h_{9/2}$  bands in  $^{187}\text{Tl}$ ,  $^{183}\text{Au}$  [9, 10], and  $^{185}\text{Au}$  [11]. Solid triangles correspond to the favoured signature, while open triangles are used for the unfavoured signature. The moment-of-inertia parameters are  $\mathcal{I}_0 = 27 \text{ MeV}^{-1}\hbar^2$  and  $\mathcal{I}_1 = 190 \text{ MeV}^{-3}\hbar^4$ .

Upon closer examination, signature splitting can be seen in the  $11/2^-$  [505] band at low spin, with the magnitude of the splitting decreasing at higher spin. Ref. [16] describes triaxial  $11/2^-$  [505] bands in  $N = 88 - 90$  nuclei that display such behaviour with  $\gamma \sim -20^\circ$  (Lund convention [17]). The loss of signature splitting at high spin can be explained as a change towards axial prolate shape caused by the alignment of a pair of  $i_{13/2}$  neutrons. We have performed potential energy surface calculations for this work (see Ref. [18] for the methodology) that predict a similar value of  $\gamma \approx -18^\circ$  for the  $11/2^-$  [505] state in  $^{187}\text{Tl}$ .

An example of a calculation assuming a coupling between the  $11/2^-$  [505] proton and a triaxial even-even core can be found in early studies on odd-mass Ir nuclei [19–21]. Their calculations approximately reproduce the experimentally observed states, providing strong evidence for the triaxiality of the  $11/2^-$  [505] state in  $^{185,187,189,191}\text{Ir}$ . Calculations for the present case of  $^{187}\text{Tl}$  are in progress.

The presence of signature splitting in the oblate  $9/2^-$  [505] and  $13/2^+$  [606] states has been interpreted in Ref. [3] as possibly being due to triaxiality, although the potential energy surface calculations predict both of these states arise from oblate, axially symmetric shapes with  $\gamma = -60^\circ$ .

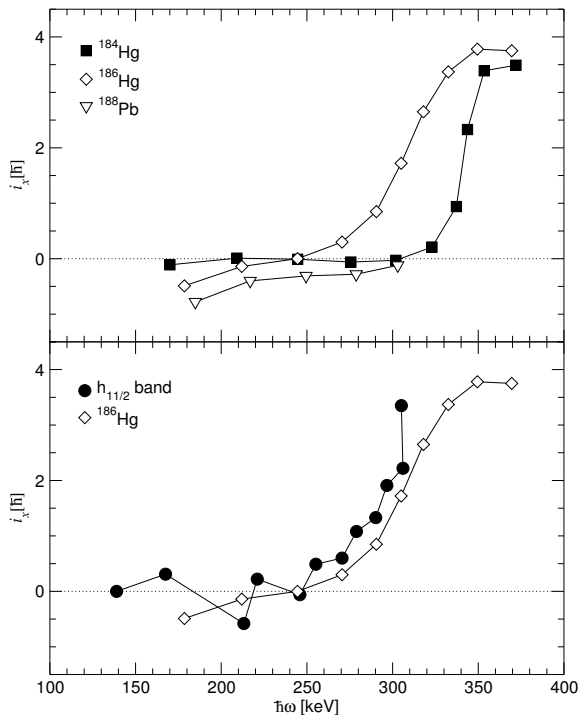


**Fig. 7.** Top panel: Alignment for the lowest prolate bands in the isotones of  $^{187}\text{Tl}$ ,  $^{186}\text{Hg}$  [13] and  $^{188}\text{Pb}$  [14], compared with their counterpart in the lighter even-even neighbour  $^{184}\text{Hg}$  [15]. Bottom panel: Alignment for the lowest prolate band in  $^{186}\text{Hg}$  compared with the alignment of the prolate  $\frac{1}{2}^-$  [505] band in  $^{187}\text{Tl}$ . The moment-of-inertia parameters are the same as those used in Ref. [12],  $\mathcal{I}_0 = 27 \text{ MeV}^{-1}\hbar^2$  and  $\mathcal{I}_1 = 190 \text{ MeV}^{-3}\hbar^4$ .

## 4 Conclusion

This paper reports on selected results from a study of  $^{187}\text{Tl}$ , in particular, new information obtained for rotational structures built upon the  $h_{9/2}$  and  $h_{11/2}$  proton states. Evidence for the unfavoured signature of the prolate  $h_{9/2}$  band is presented, based on alignment comparisons with  $h_{9/2}$  bands in  $^{183}\text{Au}$  and  $^{185}\text{Au}$  where both signatures are known. In addition, the presence of the  $11/2^-$  [505] band was confirmed, with the previously known states [3] being rearranged and the band greatly extended. The  $11/2^-$  [505] state appears to have a larger deformation than was predicted by earlier calculations, and new self-consistent calculations performed for this work predict that the  $11/2^-$  [505] state has  $\gamma = -18^\circ$ , consistent with the observation of signature splitting at low spin.

## References

1. K. Heyde and J. L. Wood, Review of Modern Physics **83**, (2011) 1467
2. W. Reviol *et al.*, Phys. Rev. C **49**, (1994) R587
3. G. J. Lane *et al.*, Nucl. Phys. A **586**, (1995) 316
4. S. K. Chamoli *et al.*, Phys. Rev. C **71**, (2005) 054324
5. A. P. Byrne *et al.*, Eur. Phys. J. A **7**, (2000) 41
6. A. B. F. Lee *et al.*, to be published
7. E. Browne and R. B. Firestone, *Table of Radioactive Isotopes*, (John Wiley & Sons, 1986)

8. F. S. Stephens, Review of Modern Physics **47**, (1975) 43
9. W. F. Mueller *et al.*, Phys. Rev. C **59**, (1999) 2009
10. L. T. Song *et al.*, Phys. Rev. C **71**, (2005) 017302
11. A. J. Larabee *et al.*, Phys. Lett. B **169**, (1986) 21
12. G. D. Dracoulis, Phys. Rev. C **49**, (1994) 3324
13. W. C. Ma *et al.*, Phys. Rev. C **47**, (1993) R5
14. G. D. Dracoulis *et al.*, Phys. Rev. C **69**, (2004) 054318
15. J. K. Deng *et al.*, Phys. Rev. C **52**, (1995) 595-603
16. S. Frauendorf and F. R. May, Phys. Lett. B **125**, (1983) 245
17. G. Anderson *et al.*, Nucl. Phys. A **268**, (1976) 205
18. F. R. Xu *et al.*, Phys. Lett. B **435**, (1998) 257
19. P. Kemnitz *et al.*, Nucl. Phys. A **245**, (1975) 221
20. J. Łukasiak *et al.*, Nucl. Phys. A **313**, (1979) 191
21. C. Schück *et al.*, Nucl. Phys. A **325**, (1979) 421